Available online at www.sciencedirect.com
SCIENCE DIRECT®
Thermochimica Acta 404 (2003) 9–17
thermochimica acta
www.elsevier.com/locate/tca

Phase diagram of mixtures of stearic acid and stearyl alcohol

François G. Gandolfo, Arjen Bot, Eckhard Flöter*

Unilever Research & Development Vlaardingen, Olivier van Noortlaan 120, 3133 AT Vlaardingen, The Netherlands

Abstract

Stearyl alcohol (98.4%), stearic acid (96.0%) and their binary mixtures were investigated by differential scanning calorimetry (DSC) at a heating and cooling rate of 10 K min^{-1}. The phase diagrams on heating and cooling were constructed and showed a eutectic behavior for the solid–liquid equilibrium line. In the heating phase diagram, the eutectic line was not always visible due to the existence of a phase transition in the solid state. A shift in the eutectic phase composition towards the acid was observed on cooling. The cooling and heating phase diagrams further differed in the fact that only two exotherms were observed during cooling where three endotherms were observed during heating. A plot of the enthalpy of the mixtures versus the mole fraction shows that different processes are involved in the solid state.

Keywords: Fatty acids; Fatty alcohols; Octadecanoic acid; Octadecanol; Solid–liquid phase transition

1. Introduction

Many food or home and personal care products are composite materials, consisting of a continuous phase and at least one dispersed phase. The dispersed phase structures the product by forming a network throughout the continuous phase. An interesting class of such structuring agents are low-molecular weight gelators of organic liquids. So-called organogels are usually prepared by dissolving the gelator (mixture) and subsequent recrystallization upon cooling [1]. The properties of these systems are controlled both by thermodynamic properties (solid–liquid equilibrium) and kinetic aspects (crystallization kinetics).

In a recent paper [2], fatty acids, fatty alcohols and their mixtures were evaluated for their oil structuring potential. Mixtures showed a synergistic effect below 20 °C at the composition ratios of 7:3 and 3:7 (w/w). This synergetic effect was most pronounced for the stearyl alcohol–stearic acid mixture. This effect was attributed to effects on the crystallization kinetics.

A lot of work has been published on Langmuir monolayers of fatty acids, fatty alcohols and their mixtures [3,4]. Mixtures of stearic acid and stearyl alcohol are miscible though non-ideality was observed both from measurements of viscosity [5] and permeability to water vapor [6]. In the “crystalline” region of the pressure–area isotherm of monolayers of mixtures of tetradecanoic acid and hexadecanol, deviation from ideality has been observed in the area/molecule at collapse point [7]. Monolayers of mixtures of heneicosanoic acid an heneicosanol were shown to be completely miscible [8–10].

The phase behavior of mixtures of fatty acids (lauric, palmitic, stearic and oleic acid) in the bulk solid phase was reported recently [11,12]. The heating and cooling phase diagrams of a fatty alcohol binary system (*n*-heptadecanol/*n*-octadecanol) with a detailed description of the solid–solid transitions were reported by Yamamoto et al. [13]. Takiguchi et al. [14] reported

* Corresponding author. Tel.: +31-10-460-5094; fax: +31-10-460-6000.
E-mail address: eckhard.floter@unilever.com (E. Flöter).

0040-6031/$ – see front matter © 2003 Elsevier Science B.V. All rights reserved.
doi:10.1016/S0040-6031(03)00086-8

that mixtures of fatty acids and fatty alcohols form a eutectic system and exhibit solid state transitions. The phase diagram of the binary behenyl alcohol–behenic acid system was given as an example. Sasin et al. [15] reported the solidification points of stearic acid–stearyl alcohol binary mixtures.

The present paper is intended to study the phase behavior of stearic acid, stearyl alcohol, and their mixtures in the solid bulk state. Characterization will take place by means of differential scanning calorimetry (DSC).

2. Experimental

2.1. Materials

Stearic acid 97% and stearyl alcohol 95% were purchased from Acros Organics. All these structuring agents were used without any further purification. The purities of stearic acid and stearyl alcohol were checked by gas chromatography analysis and were respectively 98.4 and 96.0 mol%. The abbreviations C_{18}-OH and C_{18}-acid will be used throughout this paper for respectively stearyl alcohol and stearic acid (cf. Table 1).

2.2. Methods

The phase behavior of binary mixtures of C_{18}-OH and C_{18}-acid was studied by DSC using a Perkin-Elmer Pyris 1 DSC equipped with a heating system under nitrogen circulation and a controlled cooling accessory using liquid nitrogen as cooling agent. The samples were prepared by melting the solid powders of the components followed by cooling at room temperature. In this study, 6–8 mg of sample was accurately weighted into a stainless steel sample pan. DSC-curves were recorded between 5 and 80 °C at a heating and cooling rate of 10 K min^{-1}. Some samples were investigated at a heating rate of 1 K min^{-1} to resolve the endotherms. Samples were kept 1 min at 80 °C after heating and then 1 h at 5 °C before the second heating. Heat flow data was acquired during these temperature sweeps. Overlapping endotherms or exotherms were separated using the Fraser–Suzuki algorithm in the Netzsch Peak Separation program.

3. Results and discussion

3.1. The pure components

3.1.1. Stearic acid

Stearic acid has four different crystal forms or polymorphs, A, B, C and E [16] (cf. Table 1). The C form is thermodynamically the most stable. It may be obtained by solidification of the melt and sometimes by crystallization from a polar solvent. Crystallization from a non-polar solvent usually gives either the A form or a mixture of the B and C forms. At temperatures just below the melting point, the A and B forms transform irreversibly to the C form [17]. The B and E polymorphs appear only by solution crystallization where single crystals of the E form transform to the B form [18]. The solubility curves of B and C intersect at 32 °C, which allows enantiotropy to break down with the B form becoming more stable than the C form [19].

Fig. 1a shows the cooling and second heating DSC-curves of C_{18}-acid. Only one endotherm is

Table 1
Physical properties of *n*-alcohols and *n*-fatty acids

Common name	Systematic name	Abbreviation	Polymorph	T_{fus} (°C)	$\Delta_{trs}H$ (kJ mol^{-1})
Stearic acid	Octadecanoic acid	C_{18}-acid	C	69.6[a]	61.3[a] (C → liquid)
		C_{18}-acid	B	54[b]	5.8[b] (B → C)
		C_{18}-acid	A	64[b]	
Stearyl alcohol	1-Octadecanol	C_{18}-OH	α	58.0[c]	41.1[c] (α → liquid)
		C_{18}-OH	γ	57.4[c]	25.6[c] (γ → α)

[a] Data from [25].
[b] Data from [17].
[c] Data from [20].

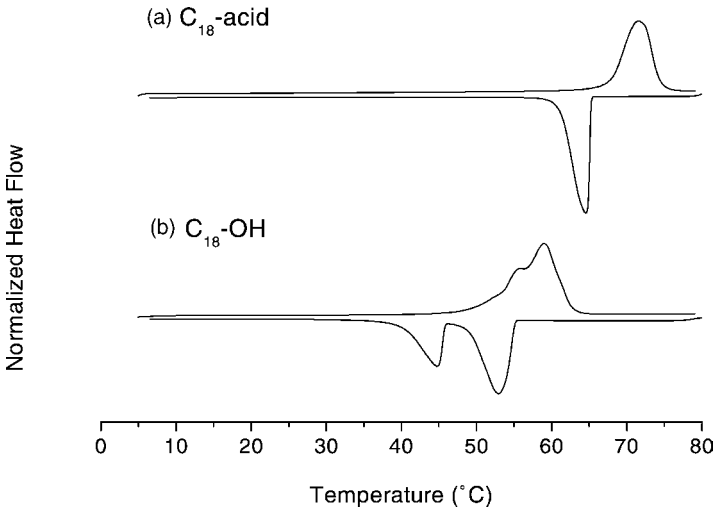

Fig. 1. DSC-curves of the pure components: (a) C_{18}-acid and (b) C_{18}-OH.

observed on heating and one exotherm on cooling. At a heating rate of 1 K min^{-1}, the endotherm has an onset melting temperature of 68.4 °C and an enthalpy of melting of 60.0 kJ mol^{-1} which is attributed to the C polymorph. These measurements are close to the 69.6 °C and 61.3 kJ mol^{-1} reported in the literature (cf. Table 1) and agree very well with published values of Cedeño et al. [11] taking into account the purity of the samples.

3.1.2. Stearyl alcohol

Straight chain, even numbered, fatty alcohols are known to crystallize as three distinct polymorphs, α, β and γ [13] (cf. Table 1). The β-form appears mainly in shorter members of the even alcohols. The polymorphs show enantiotropic behavior, with each form being thermodynamically stable in a definite range of temperatures and pressures.

Fig. 1b shows the cooling and second heating DSC-curves of C_{18}-OH. Only one endotherm with a shoulder is observed on heating and two distinct exotherms on cooling that can be resolved by peak separation. van Miltenburg et al. [20] have shown that on heating a transition occurs between the ordered phase γ and the rotator phase α, and then the α phase melts. The solid–solid phase transition, γ → α, is very close to the melting point of the α phase and thus appears as a shoulder on the curve during the heating scan. From the peak separation in the heating run, the enthalpy of the transition γ → α yielded 22.5 kJ mol^{-1}, which is close to the 25.6 kJ mol^{-1} reported in the literature (cf. Table 1). From the second cooling exotherm the enthalpy of the phase transition α → γ was determined to be −21.9 kJ mol^{-1}. This solid–solid phase transition shows a significant supercooling of 3.2 K whereas the supercooling of the liquid → α phase is very small at 0.4 K.

3.2. Binary phase diagram

3.2.1. Heating run

Fig. 2 shows some of the DSC-curves of the C_{18}-OH/C_{18}-acid binary mixtures as a function of the mole fraction of alcohol for the second heating run. The temperatures of the peak of the endotherms and enthalpies extracted from these thermograms are listed in Table 2. The binary mixtures showed one, two or even three endotherms. Upon crystallization, in general a binary mixture will form a solid solution, or an intermolecular compound or a eutectic system [21]. When ideal mixing (zero excess energy) occurs the mixture will form an ideal solid solution. In such a case, the DSC-curve for a particular mixture will be composed of one endotherm and the temperature of this endotherm will lie between the melting temperatures of the pure components. In the C_{18}-OH/C_{18}-acid binary system the melting temperatures of the endotherms go through a minimum. This

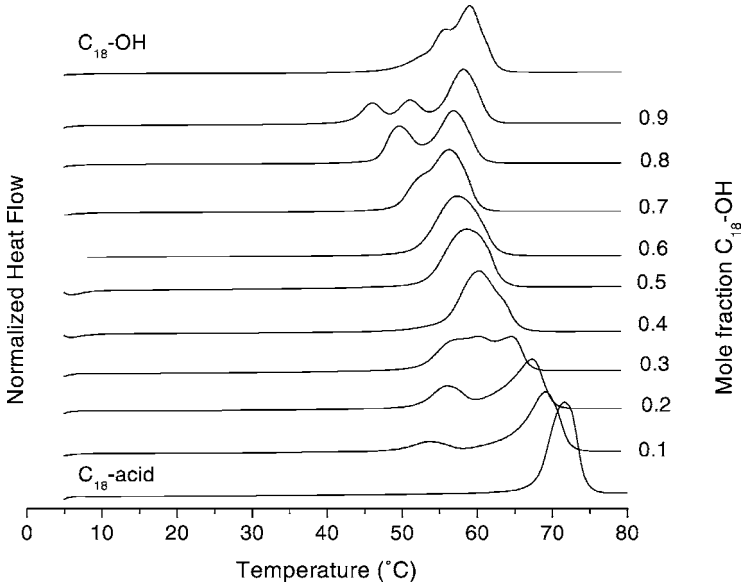

Fig. 2. DSC-curves of the C_{18}-OH/C_{18}-acid binary mixtures as a function of the weight fraction of alcohol (second heating run at $10\,K\,min^{-1}$).

Table 2
Peak temperatures and enthalpies of melting of stearic acid, stearyl alcohol and the binary mixtures (from the second heating scan)[a]

Mole fraction (C_{18}-OH)	Temperature, T_p (°C)			Peak enthalpy ($J\,g^{-1}$)			$\Delta_{fus}H$ ($J\,g^{-1}$)
	First	Second	Third	First	Second	Third	
0.00			71.6 (70.5)			211.0	211.0 (210.8)
0.05				12.5		195.8	208.3
0.10	53.4		69.2	27.0		177.6	204.6
0.15	(55.3)		(67.7)	41.9 (33.0)		167.6 (177.9)	209.5 (210.9)
0.19	56.1		67.2	47.9		160.8	208.7
0.24	(56.0)		(65.7)	50.7 (52.7)		129.5 (158.0)	211.1 (210.7)
0.29	56.0 (54.1)	59.9 (57.4)	64.8 (63.2)	51.8 (10.7)	118.1 (85.8)	38.9 (108.7)	208.8 (205.2)
0.35	56.9	60.9	65.6	21.7	165.3	26.3	213.3
0.39	59.8 (57.3)		64.1 (61.8)			208.4	208.4
0.44			61.0			214.4	214.4
0.49			58.5			209.0	209.0
0.53			58.4 (55.5)			213.2	213.2 (210.1)
0.59			57.3			214.0	214.0
0.62			57.4			215.2	215.2
0.69	51.8		56.3	18.6		197.2	215.8
0.74	52.3		58.0	49.5		165.9	215.4
0.80	50.1		57.9	74.9		139.1	214.0
0.89	46.1	51.0	58.2	38.4	47.9	129.6	215.9
0.94	43.8	53.8	59.4	13.2	92.6	114.7	220.5
1.00		55.1	58.9		83.1	143.8	226.9

[a] Data in parentheses are for experiments at a scanning rate of $1\,K\,min^{-1}$.

behavior is characteristic of a eutectic system where demixing and segregation occurs in the solid phase. In such a case, two endotherms must be present on the DSC-curves with the first endotherm appearing at a constant temperature referred to as the eutectic temperature. This eutectic behavior is observed for our system with a eutectic temperature of 56 °C as determined from mixtures with a mole fraction of stearic acid between 0.15 and 0.25. At a mole fraction of 0.1, the small endotherm appears at a temperature below the eutectic temperature which implies that C_{18}-OH is partially miscible in the stearic acid solid matrix. On the C_{18}-OH side, the first peak does not appear at a constant temperature and furthermore a third endotherm is present in the thermogram. Obviously, the solid phase transition of C_{18}-OH has an effect on the solidus line (eutectic line) of the phase diagram. Fig. 3 shows the phase diagram of the binary system as obtained by plotting the peak temperatures of the endotherms as a function of the mole fraction of alcohol. The solid–liquid equilibrium line can be modeled by using equation [22]:

$$\ln x = \frac{\Delta_{\text{fus}} H}{R}\left(\frac{1}{T_{\text{fus}}} - \frac{1}{T}\right) \quad (1)$$

also known as van't Hoff freezing point relation where x is the mole fraction of the major component at the temperature T, R the gas constant, $\Delta_{\text{fus}}H$ the molar enthalpy of fusion and T_{fus} is the melting temperature of the pure component. This equation applies to either side of a eutectic phase diagram with full miscibility and ideality in the liquid phase. A comparison of theoretical and experimental curves for the phase diagram is shown in Fig. 3. The agreement is reasonable.

Looking closer at the prediction, deviations can be noticed. The eutectic line, predicted from the intersection of the two solid–liquid equilibrium curves, is not followed in the real system due to the existence of multiple endotherms in the solid state. In order to attribute the peaks to a eutectic line or a possible solid–solid transition, the enthalpies of the various peaks were carefully analyzed in Figs. 4 and 5. The enthalpy of the eutectic endotherm is plotted versus the mole fraction of C_{18}-OH in Fig. 4. In the case of a eutectic system, the plot should show two linear portions intersecting at the eutectic composition and forming a triangle. In our system, the triangle pattern was followed for mixtures rich in C_{18}-OH or C_{18}-acid. In the middle range, a considerable deviation from the triangle pattern is observed. For compositions rich in C_{18}-acid, deviation occurs as the third endotherm appears. Deviations were more pronounced for the scanning rate of $10\,\text{K}\,\text{min}^{-1}$. At a reduced scanning rate of $1\,\text{K}\,\text{min}^{-1}$, the linear relationship between the enthalpy of the eutectic endotherm and the mole fraction of C_{18}-OH is maintained in the region with

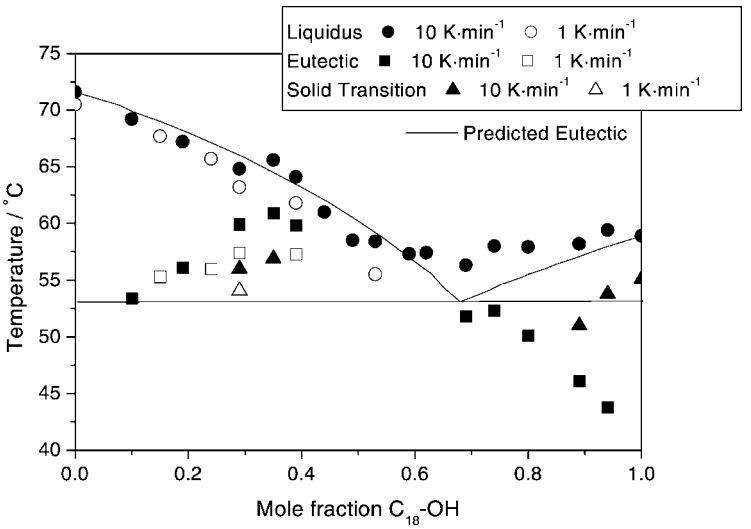

Fig. 3. Phase diagram of the binary system C_{18}-OH/C_{18}-acid for the heating run.

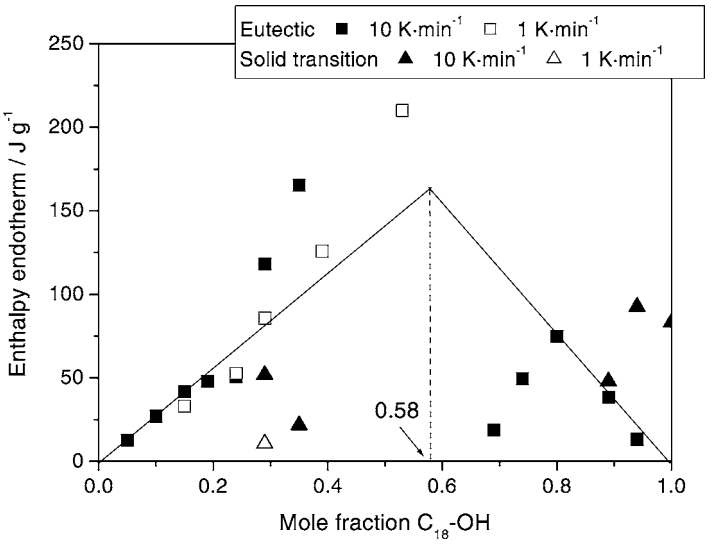

Fig. 4. A plot of the enthalpy of the endothermic events vs. the mole fraction of C_{18}-OH.

the three endotherms. At the 1 K min^{-1} scanning rate, two endotherms were clearly visible with little overlapping at the 0.29 mole fraction. In that case, the third endotherm appears as a shoulder on the left side of the first endotherm. This illustrates the fact that at 10 K min^{-1} equilibrium in the solid state was not reached for mole fractions of 0.29 and 0.35. The kinetics of the solid state transformation is a slow process. Fig. 5 shows a plot of the enthalpy of the last endotherm in joules per gram of pure component. Compositions rich in C_{18}-acid yield a plateau illustrating the fact that the endotherm is due to pure C_{18}-acid melting. A break in the plateau is observed at the mole fraction 0.29 with a different plateau level. Compositions rich in C_{18}-OH yield also a plateau and deviation is observed below a mole fraction of 0.8.

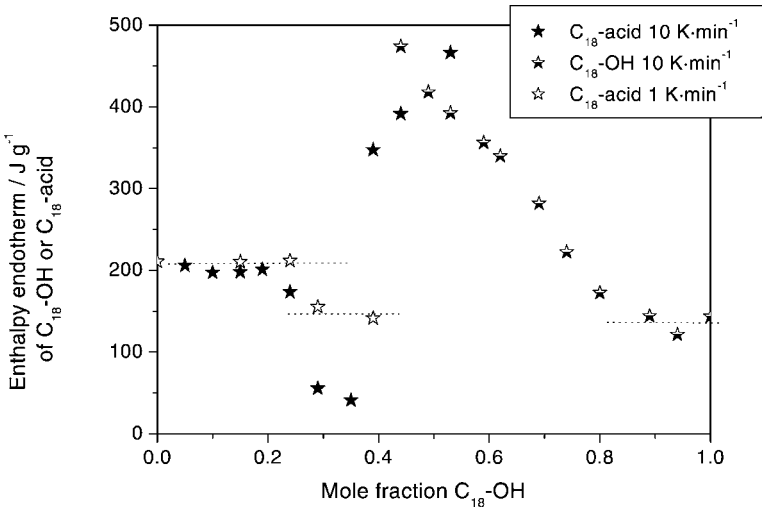

Fig. 5. A plot of the enthalpy in J g^{-1} of C_{18}-OH or C_{18}-acid for the liquidus endotherms vs. the mole fraction of C_{18}-OH.

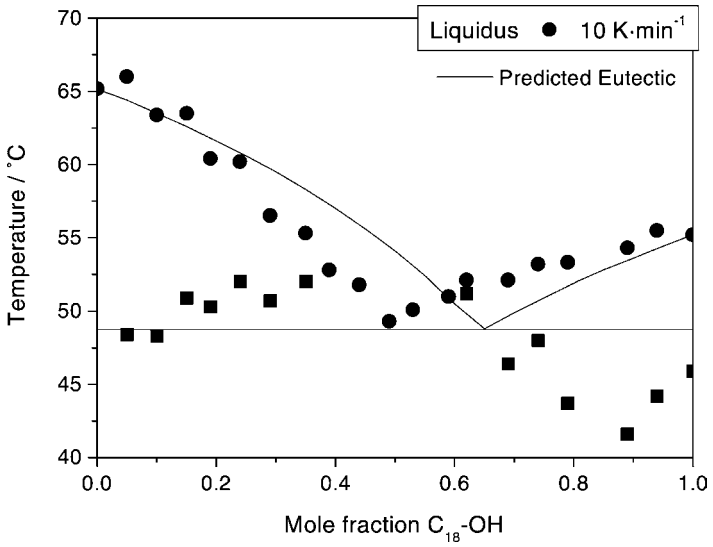

Fig. 6. Phase diagram of the binary system C_{18}-OH/C_{18}-acid for the cooling run.

3.2.2. Cooling run

Fig. 6 shows the phase diagram of the binary system as obtained by plotting the onset temperatures of the exotherms as a function of the mole fraction of alcohol for the cooling run. The onset temperatures and enthalpies of the exotherms are listed in Table 3. The binary mixtures showed either one or two exotherms upon crystallization. The phase diagram shows a eutectic behavior similar to the phase diagram of the heating run with the difference that were three endotherms were observed only two exotherms are observed in the cooling curves. A comparison of the theoretical and experimental curves for the phase diagram is also shown in Fig. 6. A clear shift of the eutectic composition towards C_{18}-acid is observed. This deviation could be due to the association of the acid molecules in the liquid as dimers. In such a case, the solubility of the acid is enhanced and the eutectic is displaced towards the associative species [23]. Fig. 7 shows a plot of the enthalpy of the eutectic exotherm versus the mole fraction of C_{18}-OH. A linear behavior is clearly observed for mixtures rich in C_{18}-acid. At a mole fraction of 0.3, where the crystallization temperature deviates from the prediction, the enthalpy of the eutectic exotherm shows a different linear behavior with an apposite slope sign. From the linearity of the enthalpy it is clear that a new process is involved

Table 3
Peak onset temperatures and enthalpies of stearic acid, stearyl alcohol and the binary mixtures (from the cooling scan)

Mole fraction (C_{18}-OH)	Temperature, T_e (°C)		Peak enthalpy ($J\,g^{-1}$)		Total enthalpy ($J\,g^{-1}$)
	First	Second	First	Second	
0.00	65.2		−208.5		−208.5
0.05	66.0	48.4	−196.1	−12.5	−208.6
0.10	63.4	48.3	−170.0	−27.8	−197.8
0.15	63.5	50.9	−160.1	−45.2	−205.3
0.19	60.4	50.3	−144.7	−60.1	−204.8
0.24	60.2	52.0	−138.7	−68.3	−207.0
0.29	56.5	50.7	−156.9	−44.8	−201.7
0.35	55.3	52.0	−161.2	−45.5	−206.7
0.39	52.8		−171.1	−31.9	−203.0
0.44	51.8		−210.4		−210.4
0.49	49.3		−202.2		−202.2
0.53	50.1		−207.5		−207.5
0.59	51.0		−208.8		−208.8
0.62	52.1	51.2	−210.3		−210.3
0.69	52.1	46.4	−156.9	−54.1	−211.0
0.74	53.2	48.0	−142.6	−70.2	−212.8
0.80	53.3	43.7	−136.5	−73.5	−212.1
0.94	54.3	41.6	−140.9	−71.2	−214.9
0.89	55.5	44.2	−137.5	−77.4	−221.7
1.00	55.2	45.9	−140.8	−80.9	−221.7

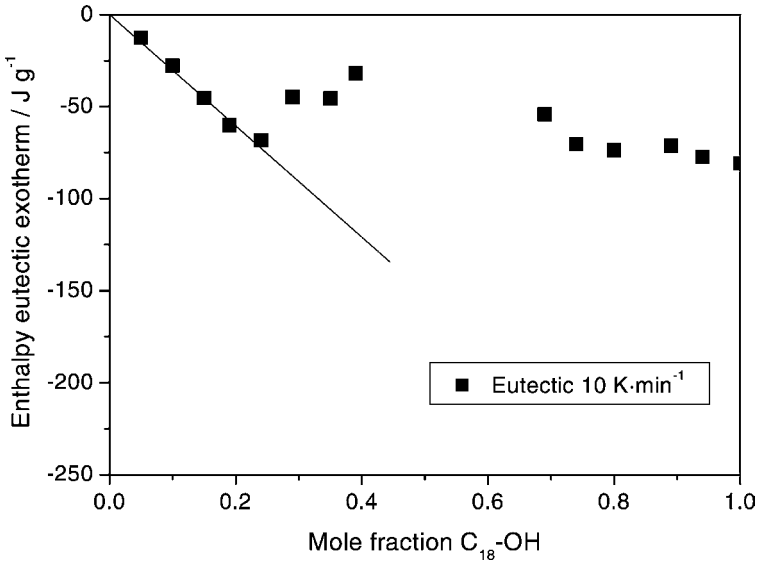

Fig. 7. A plot of the enthalpy for the eutectic exotherms vs. the mole fraction of C_{18}-OH.

at that point. On the C_{18}-OH side, no eutectic behavior is observed due to the presence of a solid–solid transformation.

4. Conclusions

The phase diagrams on heating and cooling were constructed for the stearyl alcohol/stearic acid system showing a eutectic behavior for the solid–liquid equilibrium line. Nevertheless, a closer investigation at the enthalpies of the mixtures shows a complex behavior in the solid state where differences were observed on varying the heating rate. The existence of a range of concentration where the two components possibly form a solid solution close to the eutectic composition cannot be excluded as proposed by Ralston [24].

Acknowledgements

The authors wish to thank Hans Meder (Unilever Research & Development Vlaardingen) for performing the DSC measurements. This research has been supported by a Marie Curie Fellowship of the European Community program “Human Potential” under contract number HPMI-CT-1999-00043.

References

[1] P. Terech, R.G. Weiss, Chem. Rev. 97 (1997) 3133.
[2] F.G. Gandolfo, A. Bot, E. Flöter, J. Am. Oils Chem. Soc., submitted for publication.
[3] V.M. Kaganer, H. Möhwald, P. Dutta, Rev. Modern Phys. 71 (1999) 779.
[4] H. Matuo, K. Hiromoto, K. Motomura, R. Matuura, Bull. Chem. Soc. Jpn. 51 (1978) 690.
[5] G.E. Boyd, F. Vaslow, J. Colloid Sci. 13 (1958) 275.
[6] H. Fang, D.O. Shah, J. Colloid Interface Sci. 205 (1998) 531.
[7] K. Roberts, R. Österlund, C. Axberg, J. Colloid Interface Sci. 55 (1976) 563.
[8] M.C. Shih, M.K. Durbin, A. Malik, P. Zschack, P. Dutta, J. Chem. Phys. 101 (1994) 9132.
[9] B. Fischer, E. Teer, C.M. Knobler, J. Chem. Phys. 103 (1995) 2365.
[10] E. Teer, C.M. Knobler, C. Lautz, S. Wurlitzer, J. Kildae, T.M. Fischer, J. Chem. Phys. 106 (1997) 1913.
[11] F.O. Cedeño, M.M. Prieto, A. Espina, J.R. García, Thermochim. Acta 369 (2001) 39.
[12] J.J. Zhang, J.L. Zhang, S.M. He, K.Z. Wu, X.D. Liu, Thermochim. Acta 369 (2001) 157.
[13] T. Yamamoto, K. Nozaki, T.J. Hara, J. Chem. Phys. 92 (1990) 631.
[14] H. Takiguchi, K. Iida, S. Ueno, J. Yano, K. Sato, J. Cryst. Growth 193 (1998) 641.
[15] G.S. Sasin, W.A. Butte Jr., R. Sasin, J. Am. Oils Chem. Soc. 34 (1957) 76.
[16] M. Kobayashi, in: N. Garti, K. Sato (Eds.), Crystallization and Polymorphism of Fats and Fatty Acids, Marcel Dekker, New York, 1998, p. 139.

[17] N. Garti, S. Sarig, E. Wellner, Thermochim. Acta 37 (1980) 131.
[18] F. Kaneko, K. Tashiro, M. Kobayashi, J. Cryst. Growth 199 (1999) 1352.
[19] K. Sato, in: N. Garti, K. Sato (Eds.), Crystallization and Polymorphism of Fats and Fatty Acids, Marcel Dekker, New York, 1998, p. 227.
[20] J.C. van Miltenburg, H.A.J. Oonk, L.J. Ventola, Chem. Eng. Data 46 (2001) 90.
[21] J. Visjager, T.A. Tervoort, P. Smith, Polymer 40 (1999) 4533.
[22] A. Reisman, E.M. Loebl, Phase Equilibria: Basic Principles, Applications, Experimental Techniques, Academic Press, New York, 1970, p. 130.
[23] A. Reisman, E.M. Loebl, Phase Equilibria: Basic Principles, Applications, Experimental Techniques, Academic Press, New York, 1970, p. 185.
[24] A.W. Ralston, Fatty acids and Their Derivatives, Wiley, New York, 1948, p. 373.
[25] K. Sato, N. Yoshimoto, M. Suzuki, M. Kobayashi, F. Kaneko, J. Phys. Chem. 94 (1990) 3180.